 doi:10.20944/preprints202206.0420.v1

Article

Role of Diffusion-weighted MRI in Differentiation between Benign and Malignant Anterior Mediastinal Masses

Tran Thi Mai Thuy[1,2], Nguyen Truong Hoang Trang[1,2], Tran Thanh Vy[3,4], Vo Tan Duc[1,2], Nguyen Hoang Nam[1,2], Phan Cong Chien[2], Le Huu Hanh Nhi[5] and Le Huu Nhat Minh[6,7,*]

1 Department of Radiology, University of Medicine and Pharmacy at Ho Chi Minh City, Ho Chi Minh City 700000, Vietnam
2 Department of Diagnostic Imaging, University Medical Center, Ho Chi Minh City 700000, Vietnam
3 Thoracic and Vascular Department, University Medical Center, Ho Chi Minh City 700000, Vietnam
4 Department of Thoracic and Cardiovascular Surgery, Faculty of Medicine, University of Medicine and Pharmacy at Ho Chi Minh City, Ho Chi Minh City 700000, Vietnam
5 Faculty of Medicine, University of Medicine and Pharmacy at Ho Chi Minh City, Ho Chi Minh City 700000, Vietnam
6 Emergency Department, University Medical Center, Ho Chi Minh City 700000, Vietnam
7 International Graduate Program in Medicine (IGPM), College of Medicine, Taipei Medical University, Taipei City 110, Taiwan
*Corresponding author: minh.lhn@umc.edu.vn; Tel: +84-939-759-791

Abstract: To describe the characteristics of anterior mediastinal masses on conventional magnetic resonance imaging (MRI) and to assess the role of Apparent Diffusion Coefficient (ADC) value in distinguishing benign from malignant mediastinal lesions.

We conducted a retrospective cross-sectional study in 55 patients with anterior mediastinal mass who were performed MRI before treatment. Biopsy and histopathological assessment were done after that.

The study was composed of 55 patients, with 5 bengin lesions and 50 malignant lesions. The ADC_{mean}, ADC_{median}, ADC_{10}, ADC_{90} in the histogram-based approach and hot-spot-ROI-based mean ADC for the malignant lesions was significantly lower than those found in benign lesions (P value <0.05). The hot-spot-ROI-based mean ADC had the highest value in differentiation between benign and malignant mediastinal lesions, between group A (benign lesions, thymoma A, AB, B1) and group B (thymoma B2, B3 and other malignant lesions). The cut off point (with sensitivity, specificity) of the ADC value differentiating malignant from benign mediastinal lesions; differentiating group A from group B were $1.17x10^{-3}mm^2/s$ (80%, 80%); $0.99 x10^{-3}mm^2/s$ (78.4% and 88.9%) respectively.

Diffusion weighted MRI and measurement of ADC value in histogram-based approach and hot-spot-ROI-based mean ADC are very helpful in the differentiation between benign and malignant anterior mediastinal lesions.

Keywords: anterior mediastinal lesions; diffusion weighted imaging; diffusion magnetic resonance imaging; gadolinium; thyroma; lymphoma; thymus neoplasms; biopsy

1. Introduction

Mediastinal masses are relatively rare entities which present a diverse array of histopathology, ranging from benign lesions to malignancies. Normally, the anterior mediastinum contains the thymus, lymph nodes, fat tissue, nerves, blood vessels, and sometimes the thyroid gland descending from the neck. Masses in the anterior compartment of mediastinum are often originated from these structures [1].

Imaging plays a pivotal role in establishing the initial diagnosis and guiding the selection of supplementary tests needed to reach the final diagnosis. Because of superior soft tissue contrast, MRI is considered an ideal tool for evaluating mediastinal masses.

 doi:10.20944/preprints202206.0420.v1

Preoperative assessment of the involvement of the lesion with the pericardium, heart, spinal cord, and blood vessels is a common indication. In addition, non-contrast MRI is an alternative to evaluate mediastinal masses in patients who have contraindications to intravenous contrast. Chemical shift imaging has been shown to be useful in differentiating normal thymus and thymic hyperplasia from thymic neoplasms and lymphoma. Diffusion MRI is a novel technique which is able to assess physiologic differences between tissues based on random motion of water protons [2]. On diffusion-weighted pulse sequences, the motion causes scattering of spins resulting in signal loss. This signal loss can be quantified by calculating the ADC, which reflects the specific diffusion capacity of biological tissue. The presence of diffusion obstacles such as cell membranes, tight junctions, macromolecules, cell organelles and the movement of water protons will lead to decreased ADC. It is hypothesized that hypercellular tumors have low ADC value; whereas tissues with lower cell density (necrotic tissue, non-neoplastic tissue, etc.) have higher ADC values. Therefore, ADC value can be used to distinguish necrotic tissue and benign lesions from malignancies. The cellular structure of a tumor is considered an indicator of its progression and response to treatment. In malignant lesions, the extracellular space is markedly narrowed due to increased cellularity, cell volume and impaired cell membranes. Rapidly growing tumors have increased quantity of organelles and cytoskeleton. The increase in cellular density and microstructures will in turn restrict the movement of water molecules [3,4].

Although there have been several studies on the role of MRI in evaluating anterior mediastinal lesions, its value is still controversial. Some researches show that diffusion-weighted imaging is valuable in differentiating between benign and malignant anterior mediastinal lesions. This study was carried out with the aims of characterising anterior mediastinal masses on conventional and diffusion MRI, and evaluate the role of diffusion MRI in differentiating benign and malignant anterior mediastinal tumors.

2. Materials and Methods

This is a retrospective cross-sectional study including 55 patients with anterior mediastinal tumors, who underwent preinterventional chest MRI at University Medical Center Ho Chi Minh City from September 2018 to June 2021. The tumors were then pathologically examined with samples taken from operation or biospy. Tumors without solid components or recurrent cases were excluded from the sample. Most cases underwent MRI to detect thymic lesions in patients with myasthenia gravis, and to evaluate local invasion of the tumors to heart, pericardium, large blood vessels.

All studies were performed on a 3 T MR unit (Magnetom, Siemens, Germany) at University Medical Center Ho Chi Minh City. The MRI protocol for each patient included T2 HASTE, T2 HASTIRM, DWI, T1 VIBE DIXON before and after Gadolinium injection, with the following parameters. Axial T2 HASTE: TR =1000 ms, TE = 92 ms, slice thickness: 6 mm, field of view: 260x360 and matrix: 240x320. Sagittal T2 HASTE: TR = 600 ms, TE = 27 ms, slice thickness: 8 mm, field of view: 350x350 and matrix: 256x320. Coronal T2 HASTE: TR = 600 ms, TE= 26 ms, slice thickness: 8 mm, field of view: 400x400 and matrix: 256x320. Axial T2 HASTIRM: TR = 1600 ms, TE= 86 ms, slice thickness: 6.5 mm, field of view: 300x380 and matrix: 260x320. Axial T1 opphase: TR = 4.2 ms, TE= 1.3 ms, slice thickness: 3 mm, field of view: 280x380 and matrix: 240x320. Axial T1 inphase: TR = 4.2 ms, TE = 2.6 ms, slice thickness: 3 mm, field of view: 280x380 and matrix: 240x320. Axial DWI: TR = 6500 ms, TE = 72 ms, slice thickness: 6 mm, field of view: 320x400 and matrix: 120x150. Diffusion-weighted images were obtained by using a echo-planar imaging sequence with b values of 0 and 2000 s/mm^2. ADC maps were constructed by the machine's software and displayed simultaneously after DWI images were acquired.

MRI results were examined on PACS system at University Medical Center Ho Chi Minh City. The characteristics investigated include: size, border, presence of necrotic or cystic component, presence of lesional fat. These characteristics are analysed based on T1W DIXON images before and after Gadolinium injection, T2 HASTE, T2 TIRM.

Preprints (www.preprints.org) | NOT PEER-REVIEWED | Posted: 30 June 2022 doi:10.20944/preprints202206.0420.v1

Quantification of ADC values of solid component was acquired with b values of 0 and 2000 s/mm^2. Chemical shift imaging has been proved to be highly valuable in determining the fat composition of a lesion or an organ [9]. In order to accurately quantify the presence of fat, we used the SII, which stands for Signal Intensity Index. Fat composition was determined by comparing the signal intensity of the lesion on in- and out-of-phase T1-weighted images. ROI (Region of Interest) was placed on the slice with the largest tumor area with ROI area occupying approximately three fourths of tumor. The SII was calculated by the formula:

$$SII = \frac{(tSI_{in} - tSI_{op})\text{-}}{tSI_{in}} \; x \; 100$$

Regions of interest were manually placed on the ADC map at 3 different sites of solid tissue which had the lowest signals (ROI area of 0.5 cm^2). Areas of fat, hemorrhage, necrosis, and cystic components were excluded from the ROI. The average of three ADC values was then obtained. For whole-tumor histogram analysis of ADC maps, we used Firevoxel, which is a software developed by Center for Biomedical Imaging, Department of Radiology, New York University. ROI was manually drawn on each slice. Large areas of fat, necrosis, cysts, and hemorrhage were removed from the ROI area. Eventually, the software constructed the histogram analysis of ADC values, including ADC mean, ADC median, 10th and 90th percentile of ADC.

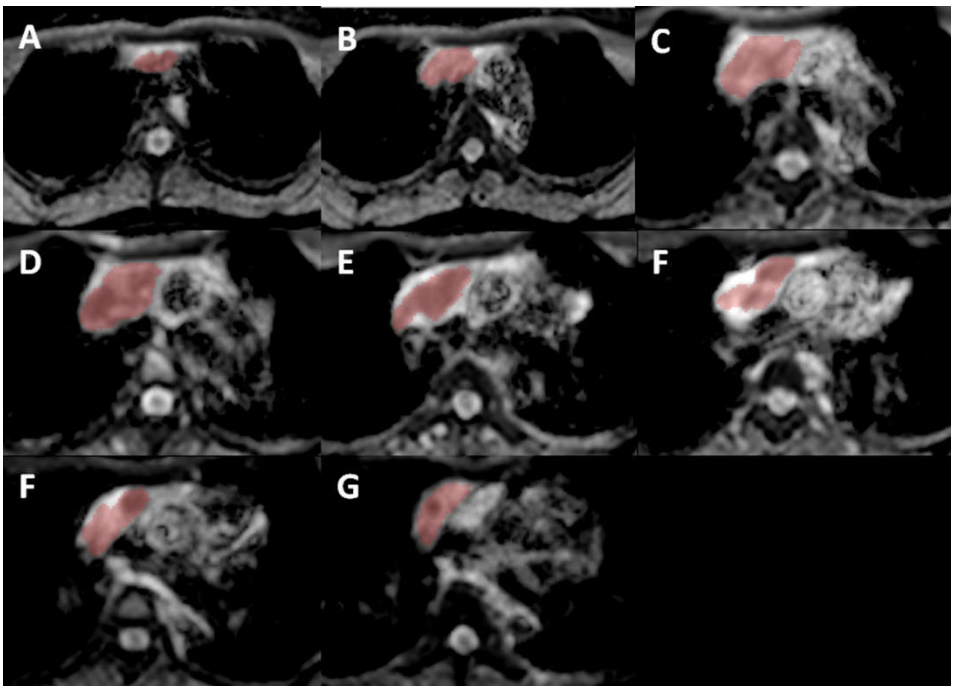

Figure 1. Whole-tumoral ROI was manually placed on the ADC map by using Firevoxel.

Preprints (www.preprints.org) | NOT PEER-REVIEWED | Posted: 30 June 2022 doi:10.20944/preprints202206.0420.v1

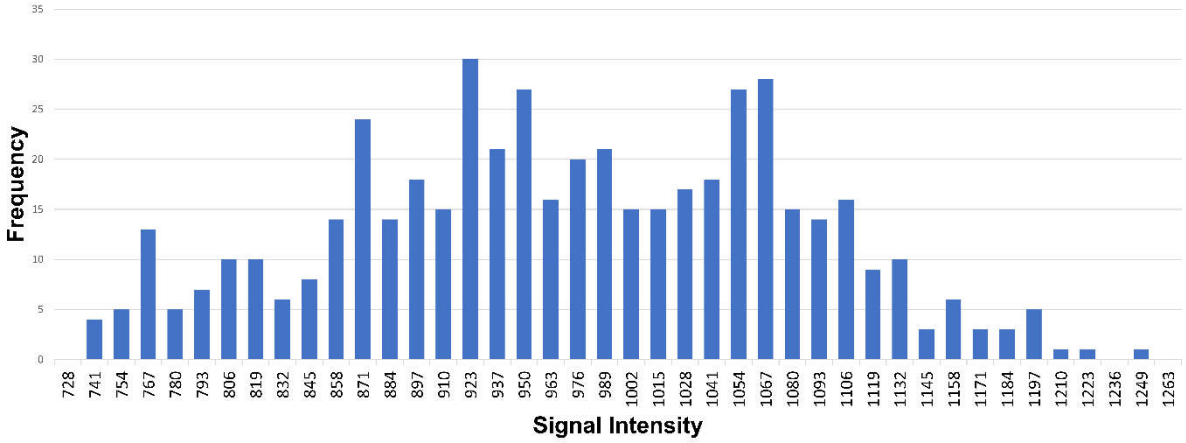

Figure 2. An example of whole-tumor histogram analysis of the ADC map.

A 35-year-old female patient with primary mediastinal large B-cell lymphoma.

Additionally, we divided the anterior mediastinal tumors into two groups in two different ways: group A (including benign tumors and type A, AB, B1 thymoma) and group B (including type B2, B3 thymoma and other malignancies); lymphoma and other malignancies. Datas are shown as frequency and percentage for qualitative variables; for normally distributed quantitative variables, datas are shown as mean values and standard deviation; for non-normally distributed quantitative variables, datas are shown as median and interquartile range. We used chi-squared and Fisher's tests to compare proportions. Mann–Whitney test was used to compare non-normally distributed means. Receiver operating characteristic curve was drawn to detect the cutoff ADC value with calculation of sensitivity, specificity, negative predictive value, positive predictive value. The data were analysed with STATA version 14.1 (STATA Corp., Texas, USA). P values of 0.05 or less indicated statistical significance.

3. Results

Our study included 55 patients (23 male, 32 female) with 5 benign lesions (9.1%) and 50 malignant lesions (90.9%). The pathological diagnostics of benign lesions were thymic hyperplasia, teratoma and Castleman disease. High risk thymoma had the highest rate in malignant group (32%). Pathological diagnostics are presented in Table 1.

Table 1. Pathological diagnostics.

Pathology	Quantity	Rate
Benign tumor	***5***	
Thymic hyperplasia	2	40%
Teratoma	2	40%
Castleman disease	1	20%
Malignant tumor	***50***	
Low risk thymoma	13	26%
High risk thymoma	16	32%
Thymic carcinoma	8	16%
Thymic NET	2	4%
Malignant germ cell tumor	4	8%
Lymphoma	7	14%

The mean age of benign group was 26.8 ± 10.5 (range 13-37). The mean age of malignant group was 49.5 ± 16.4 (range 15-82). Out of benign lesions, teratoma had the largest diameter of 114.5 mm, Castleman disease had the smallest diameter of 36 mm. Out of

Preprints (www.preprints.org) | NOT PEER-REVIEWED | Posted: 30 June 2022 doi:10.20944/preprints202206.0420.v1

malignant lesions, malignant germ cell tumor had the largest diameter of 124.8 mm, low risk thymoma had the smallest diameter of 54.2 mm. Thymic hyperplasia and Castleman disease had regular margins and no cystic component. Tumors derived from germ cell (teratoma, malignant germ cell tumor) all contained cystic component and had lobulated margin. Among thymic epithelial tumors (low risk thymoma, high risk thymoma and thymic carcinoma), rate of lesions containing fluid and having lobulated margin increased correspondingly to the degree of malignancy. Most of lymphoma did not contain fluid, and have quite equal rates between lobulated margin lesions and regular margin lesions. Thymic hyperplasia and teratoma had high SII, 60.5% and 41.7% respectively. Other tumors have low SII, range from -5.1 to 7.4. Table 2 summarizes the detailed relationship between MRI findings and pathological diagnostics.

Table 2. Relationship between MRI findings and pathological diagnostics.

Pathology	Diameter [1] (mm)	Margin [2]		Cystic [2]		SII [1]
		Regular	Lobulated	No	Yes	
Benign (N=5)	***73.4 ± 39.3***					
Thymic hyperplasia	49.5 ± 7.8	2 (100)	0	2 (100)	0	60.5 ± 44.2
Teratoma	114.5 ± 20.5	0	2 (100)	0	2 (100)	41.7 ± 6.4
Castleman disease	39	1 (100)	0	1 (100)	0	-5.1
Malignant (N=50)	***71.9 ± 32.3***					
Low risk thymoma	54.2 ± 20.7	10 (76.9)	3 (23.1)	9 (69.2)	4 (30.8)	7.4 ± 17.8
High risk thymoma	63.4 ± 31.7	6 (37.5)	10 (62.5)	11 (68.7)	5 (31.3)	-0.8 ± 6.5
Thymic carcinoma	74.6 ± 19.2	1 (12.5)	7 (87.5)	4 (50)	4 (50)	2.6 ± 5.3
Thymic NET	88.5 ± 24.7	0	2 (100)	0	2 (100)	-4.3 ± 9.1
Malignant GCT	124.8 ± 35.1	0	4(100)	0	4 (100)	1.4 ± 3.9
Lymphoma	86.1 ± 30.7	3 (42.9)	4 (57.1)	6 (85.7)	1 (14.3)	0.5 ± 4.7

[1] In diameter and SII, data are reported as mean ± standard deviation

[2] In margin and cystic, data are reported as quantity (percent)

SII: Signal intensity index NET: Neuroendocrine tumor GCT: germ cell tumor

The differences in hot-spot-ROI-based mean ADC between benign and malignant, group A and B, lymphoma and other malignant tumors were statistically significant. Group B exhibited significantly lower ADC10, ADCmedian, ADCmean, and ADC90 ($p < 0.05$) compared to group A.There were no significant differences in the ADC10, ADCmedian, ADCmean and ADC90 between benign and malignant tumors, lymphoma and other malignant tumors ($p > 0.05$).

Table 3 shows ADC values of different benign and malignant mediastinal lesions obtained by two approaches: hot-spot ROI and whole-lesion histogram.

Preprints (www.preprints.org) | NOT PEER-REVIEWED | Posted: 30 June 2022 doi:10.20944/preprints202206.0420.v1

Table 3. Hot-spot-ROI-based . nd Histogram-based ADC measurements.

Pathology	Mean ADC ($x10^{-3}mm^2/s$)	Histogram-based ($x10^{-3}mm^2/s$)			
		ADC_{mean}	ADC_{median}	ADC_{10}	ADC_{90}
Benign (N=4)					
Thymic hyperplasia	1.47 ± 0.34	1.33 ± 0.12	1.34 ± 0.16	1.08 ± 0.05	1.55 ± 0.17
Teratoma	1.46 ± 0.2	1.24 ± 0.01	1.23 ± 0.04	0.99 ± 0.16	1.52 ± 0.21
Castleman disease	0.8	0.84	0.82	0.7	1.05
Malignant (N=43)					
Low risk thymoma	1.19 ± 0.18	1.2 ± 0.2	1,2 ± 0.2	0.97 ± 0.2	1,45 ± 0,2
High risk thymoma	0.98 ± 0.36	1.05 ± 0.28	1.06 ± 0.29	0.81 ± 0.24	1.3 ± 0.31
Thymic carcinoma	0.9 ± 0.17	0.93 ± 0.15	0.93 ± 0.15	0.74 ± 0.14	1.12 ± 0.17
Thymic NET	0.6 ± 0.04	0.83 ± 0.04	0.82 ± 0.04	0.63 ± 0.03	1.03 ± 0.03
Malignant GCT	0.8 ± 0.16	1.1 ± 0.17	1.08 ± 0.16	0.82 ± 0.09	1.33 ± 0.19
Lymphoma	0.75 ± 0.12	0.95 ± 0.16	0.94 ± 0.17	0.76 ± 0.13	1.16 ± 0.2

Data are reported as mean ± standard deviation
ADC: Apparent diffusion coefficient NET: Neuroendocrine tumor GCT: germ cell tumor

ROC curves were drawn to determine the diagnostic value of hot-spot-ROI-based mean ADC and the histogram parameters for differentiating benign lesions and malignant lesions, group A and group B, lymphoma and other malignant tumors, with calculation of the cutoff value, sensitivity, specificity, and area under the ROC curve (AUC). Results are presented in table 4.

Table 4. Diagnostic Ability of Histogram-Based and Hot-Spot-ROI-Based ADC Measurements for differentiation between malignant and benign, A and B, Lymphoma and other malignan tumors.

Benign and malignant		**AUC**	**Cut-off**	**Sensitivity**	**Specificity**	**Accuracy**
Mean ADC		0.794	1.17	80	80	80
Group A and B		**AUC**	**Cut-off**	**Sensitivity**	**Specificity**	**Accuracy**
Mean ADC		0.843	0.99	78.4	88.9	81.8
Histogram-based approach	**ADCmean**	0.755	1.04	64.9	83.3	70.9
	ADCmedian	0.752	1.03	64.9	83.3	70.9
	ADC10	0.758	0.85	75.7	72.2	74.6
	ADC90	0.755	1.22	62.2	88.9	70.9
Lymphoma and other malignant tumors		**AUC**	**Cut-off**	**Sensitivity**	**Specificity**	**Accuracy**
Mean ADC		0.772	0.91	100	60.5	66

ADC: Apparent diffusion coefficient

Mean ADC value based on hot-spot-ROI with the cutoff value of 1.17 had the highest sensitivity, specificity, accuracy in differentiating groups of tumors above. Out of ADC values obtained from whole-tumor histogram analysis, ADC10 was the most valuable in differential diagnostic, followed by ADCmean, ADC90 and ADCmedian. (Figure 3)

Preprints (www.preprints.org) | NOT PEER-REVIEWED | Posted: 30 June 2022 doi:10.20944/preprints202206.0420.v1

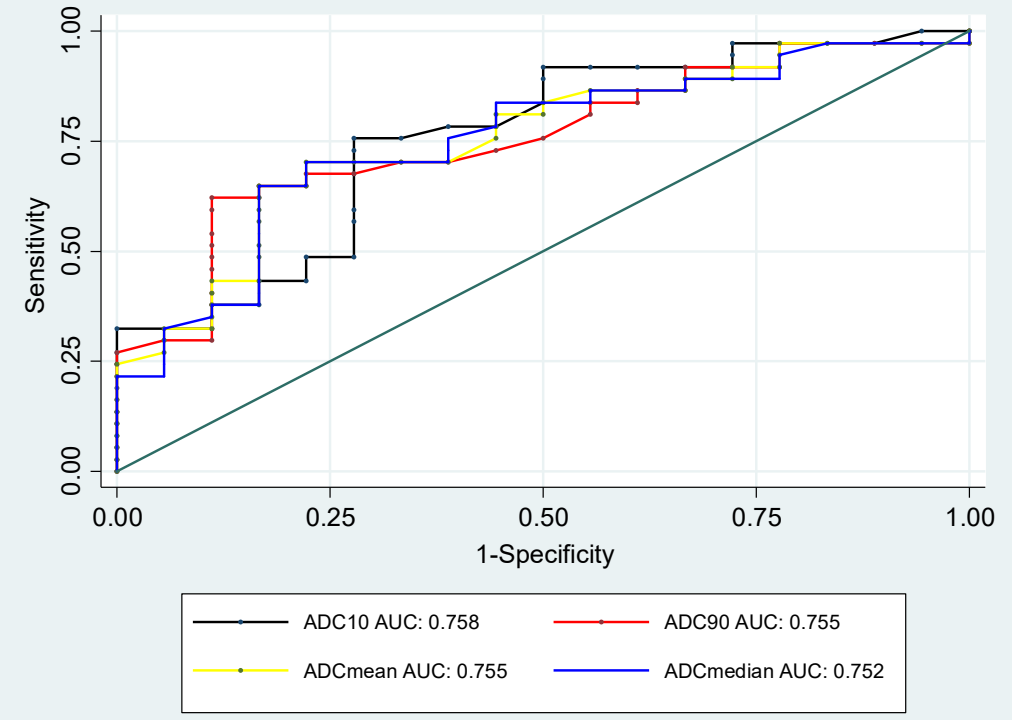

Figure 3. ROC curves of histogram-based ADC measurements for differentiating between A and B.

4. Discussion

The findings of the largest diameter, contour and cystic component of anterior mediastinal tumors in our study were quite similar to macroscopic appearance as well as radiographic features of these tumors described in textbooks [5-7].

Our study showed that average SII of thymic hyperplasia was 60.5%, and this result was close to the result of M. Priola et al, in which the average SII of thymic hyperplasia was 45.9% [8]. The mean SII value of teratoma was 41.7%, which was correlated well with the fat component in these lesions. Academically, macroscopic and microscopic appearance of Castleman disease and malignant tumors in anterior mediastinum show no fat component, and the low average SII of these lesions in our study demonstrated that fact as well. The low SII of malignant tumors in our study was also similar to the result of M. Priola et al [8]. M. Priola et al reported that SII was perfectly used to distinguish malignant tumors from thymic hyperplasia with the cut-off point of 8.92% (sensitivity and specificity 100%), and no overlap was found for SII between groups [8]. However, in our study, one case pathologically diagnosed as sclerosing thymoma, had a high SII value, which was overlapped with SII values in teratoma and thymic hyperplasia groups. It can be explained that when placing a ROI within the tumor to determine SII value, we accidentally chose the area having both tumoral tissue and normal thymic tissue, so that fat in normal thymic tissue raised the SII value. Similarly, there was a case report of a sclerosing thymoma by Li Xin et al, the surgical specimen of this case contained adipose tissue, imperfect degradation of thymus tissue and tumor components [9]. If the SII value of sclerosing thymoma was the outlier, there would be no overlapped values between teratoma, thymic hyperplasia group and other tumors group.

Preprints (www.preprints.org) | NOT PEER-REVIEWED | Posted: 30 June 2022 doi:10.20944/preprints202206.0420.v1

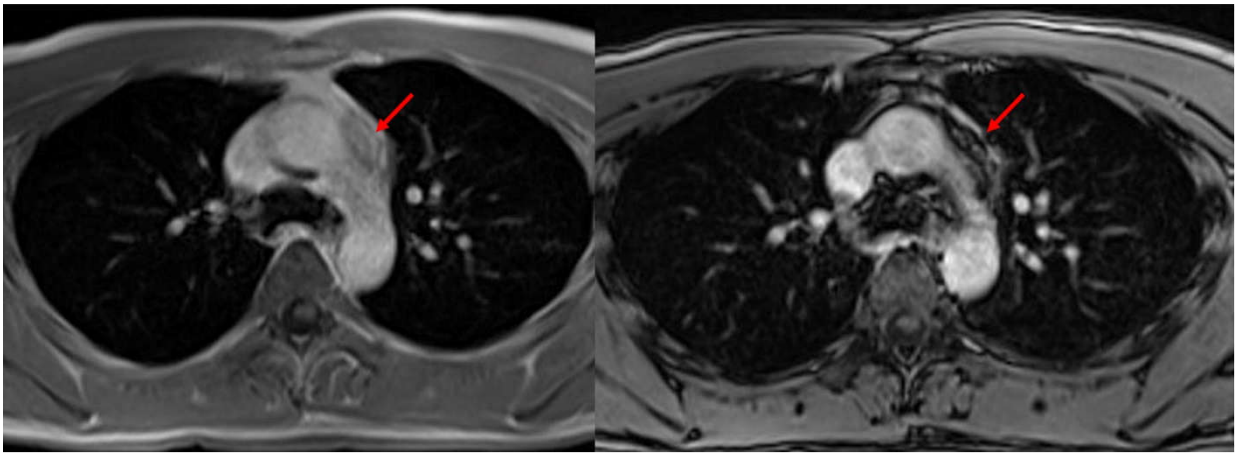

Figure 4. Sclerosing thymoma.

A 27-year-old male patient with with an anterior mediastinal mass. Placing a ROI in A (inphase) and B (opphase) with the same position and area to identify SII. SII was calculated and the result was 64,6%. The pathological result was sclerosing thymoma.

When using the hot-spot approach, the mean ADC to distinguish malignant from benign tumors was 1.17 x10^{-3}mm^2/s, with the area under curve ROC was 0.794, sensitivity and specificity were 80%. This result is concordant with that of Raafat et al who revealed that the cut-off ADC value for the differentiation between malignant and benign mediastinal lesions was 1.11 x10^{-3}mm^2/s, with sensitivity of 90.9% and specificity of 100% [10]. However, our result is discordant with Usuda et al, who reported higher cut-off value of 2.21 x10^{-3}mm^2/s for the discrimination between malignant and benign mediastinal tumors [11]. The differences in sample size and ADC mesurement method between our study and Usuda's may lead to the distinction of the two results. There were some cystic lesions in Usuda's study, whereas our study excluded the cystic lesions. In addition, when mesuring the ADC values, Usuda et al placed a ROI around the margin of the tumor without excluding fatty, necrotic, cystic and hemorrhagic areas, leading to the higher ADC values.

When comparing the hot-spot-ROI-based mean ADC between group A and B, the results of our study demonstrated that the mean ADC value of group B was significantly lower than the mean ADC value of group A, with the cut-off point of 0.99 x10^{-3}mm^2/s, sensitivity, specificity, accuracy were 78.4%, 88.9% and 81.8% respectively. In agreement with our study, Nars et al reported cut-off value of 1.15 x10^{-3}mm^2/s, sensitivity was 95%, specificity was 93.8% and accuracy was 94.4% [2]. However, this was discordant with Razek et al and Gumustas et al, they both reported higher cut off ADC value of 1.56 x10^{-3}mm^2/s and 1.39 x10^{-3}mm^2/s [12,13].

In agreement with Zhang et al, who reported that mean ADC of lymphoma was significantly lower than the mean ADC of thymic carcinoma, our study showed that the hot-spot-ROI-based mean ADC value of lymphoma was significantly lower than the mean ADC value of other malignant mediastinal tumors, with the cut-off point was 0.91 x10^{-3}mm^2/s. However, Zhang et al reported the lower cut-off ADC value of 0.73 x10^{-3}mm^2/s [9]. This variation of cut-off ADC values is likely attributed to the discrepancy in the sample size. Our result was discordont with Razek et al, Gumustas et al, Sabri et al, they were all reported that there was no significant difference in the mean ADC value between lymphoma and other malignant tumors [12-14].

When whole-lesion histograms were used to derive ADC parameters, our study showed that ADC10, 90, mean, median in group B were significantly lower than those in group A. ADC10 demonstrated a significantly better performance, when using ADC10 = 0.85 x10^{-3}mm^2/s as the cut-off value, the optimal distinction could be obtained, with sensitivity was 75.7%, specificity was 72.2% and accuracy was 74.6%. This was quite similar to the result of Zhang et al, who reported that ADC10 was superior to mean, median or 90th percentile ADC in differentiating tumors [9]. In agreement with our result, Kong et al

demonstrated that ADC10 showed best differentiating ability for discriminating low-risk thymoma from high-risk thymoma and thymic carcinoma [9]. Huang et al found that ADC10 was helpful in WHO grading of ependymoma [15]. Similarly, Donati et al showed that ADC10 correlated with Gleason score better than the other ADC did, suggesting that the 10th percentile ADC may be the best for distinguishing low- from intermediate- or high-grade prostate cancer [16]. Within a tumor with heterogeneous cellularity, focal areas with high cellularity were represented to a greater extent by the low percentile ADCs than mean or median ADCs. [17]. Therefore, it was easy to understand why ADC10 demonstrated a better differentiating performance.

Our study had some limitations. First, the sample size was small. Second, there was a wide spectrum of diseases and histopathological types in our study. Further studies focusing on specific tumor types with large sample size are recommended.

5. Conclusion

Chemical shift MRI is valuable for determining the fatty component of lesions and organs. We suggested that diffusion weighted MRI with ADC measurements may help in differentiating malignant tumors from benign tumors, lymphoma from other malignant tumors in anterior mediastinum and hot-spot-based-ROI mean ADC was the most useful value in distinguishing these groups of tumors.

Author Contributions: Conceptualization, Tran Thi Mai Thuy and Vo Tan Duc; Data curation, Tran Thi Mai Thuy and Nguyen Hoang Nam; Formal analysis, Tran Thi Mai Thuy, Phan Cong Chien and Le Huu Nhat Minh; Investigation, Tran Thi Mai Thuy, Nguyen Truong Hoang Trang, Tran Thanh Vy and Phan Cong Chien; Methodology, Tran Thi Mai Thuy; Project administration, Tran Thi Mai Thuy and Le Huu Nhat Minh; Software, Vo Tan Duc, Phan Cong Chien and Le Huu Nhat Minh; Supervision, Vo Tan Duc and Le Huu Nhat Minh; Validation, Le Huu Nhat Minh; Writing – original draft, Tran Thi Mai Thuy, Nguyen Truong Hoang Trang, Tran Thanh Vy, Vo Tan Duc, Nguyen Hoang Nam, Phan Cong Chien, Le Huu Hanh Nhi and Le Huu Nhat Minh; Writing – review & editing, Nguyen Hoang Nam, Le Huu Hanh Nhi and Le Huu Nhat Minh.

Funding: This research received no external funding.

Institutional Review Board Statement: The study was conducted in accordance with the Declaration of Helsinki, and approved by the In-stitutional Review Board of University Medical Center, Ho Chi Minh City (protocol code 739/HDDD-DHYD, date of approval: 20 October 2020).

Informed Consent Statement: Informed consent was waived because of the retrospective nature of the study and the analysis used anonymous clinical data.

Data Availability Statement: Not applicable.

Acknowledgments: The authors wish to express their sincere gratitude for their cooperation to the staff of the Forest Service of Xanthi. This synergy contributed to a great extent to the implementation of the current research project. We hope that the research will contribute to the existing body of knowledge and raise awareness among forest managers. The authors also wish to thank Mrs. Malivitsi Zoe for editing the paper.

Conflicts of Interest: The authors declare no conflict of interest.

References

1. Almeida, P.T.; Heller, D. Anterior Mediastinal Mass. *StatPearls [Internet]* **2019**.
2. Nasr, A.; Elshahat, H.; Safwat, H.; Alsaif, R.; Alshehab, D.; Shebl, M. Diffusion weighted MRI of mediastinal masses: Can measurement of ADC value help in the differentiation between benign and malignant lesions. *The Egyptian Journal of Radiology and Nuclear Medicine* **2016**, *47*, 119-125.
3. Herneth, A.M.; Guccione, S.; Bednarski, M. Apparent diffusion coefficient: a quantitative parameter for in vivo tumor characterization. *European journal of radiology* **2003**, *45*, 208-213.
4. Sabri, Y.Y.; Kolta, M.F.F.; Khairy, M.A. MR diffusion imaging in mediastinal masses the differentiation between benign and malignant lesions. *The Egyptian Journal of Radiology and Nuclear Medicine* **2017**, *48*, 569-580.
5. Burke, A.P.; Aubry, M.-C.; Maleszewski, J.; Alexiev, B.; Tavora, F. *Practical thoracic pathology: diseases of the lung, heart, and thymus*; Lippincott Williams & Wilkins: 2016.
6. Suster, S.; Moran, C.A. *Diagnostic Pathology: Thoracic E-Book*; Elsevier Health Sciences: 2017.

7. Travis, W.D.; Brambilla, E.; Muller-Hermelink, H.K.; Harris, C.C. World Health Organization classification of tumours. *Pathology and genetics of tumours of the lung, pleura, thymus and heart* **2015**, *10*, 183-280.
8. Priola, A.M.; Priola, S.M.; Ciccone, G.; Evangelista, A.; Cataldi, A.; Gned, D.; Pazè, F.; Ducco, L.; Moretti, F.; Brundu, M. Differentiation of rebound and lymphoid thymic hyperplasia from anterior mediastinal tumors with dual-echo chemical-shift MR imaging in adulthood: reliability of the chemical-shift ratio and signal intensity index. *Radiology* **2015**, *274*, 238-249.
9. Kong, L.-Y.; Zhang, W.; Zhou, Y.; Xu, H.; Shi, H.-B.; Feng, Q.; Xu, X.-Q.; Yu, T.-f. Histogram analysis of apparent diffusion coefficient maps for assessing thymic epithelial tumours: correlation with world health organization classification and clinical staging. *The British journal of radiology* **2018**, *91*, 20170580.
10. Raafat, T.A.; Ahmed, S.M.; Seif, E.M.A.; Mikhael, H.S.W.; Awad, A.S. Role of diffusion-weighted MRI in characterization of mediastinal masses. *Egyptian Journal of Radiology and Nuclear Medicine* **2020**, *51*, 1-12.
11. Usuda, K.; Maeda, S.; Motono, N.; Ueno, M.; Tanaka, M.; Machida, Y.; Matoba, M.; Watanabe, N.; Tonami, H.; Ueda, Y. Diffusion weighted imaging can distinguish benign from malignant mediastinal tumors and mass lesions: Comparison with positron emission tomography. *Asian Pacific Journal of Cancer Prevention* **2015**, *16*, 6469-6475.
12. Gümüştaş, S.; İnan, N.; Sarisoy, H.T.; Anik, Y.; Arslan, A.; Çiftçi, E.; Akansel, G.; Demirci, A. Malignant versus benign mediastinal lesions: quantitative assessment with diffusion weighted MR imaging. *European radiology* **2011**, *21*, 2255-2260.
13. Razek, A.A.; Elmorsy, A.; Elshafey, M.; Elhadedy, T.; Hamza, O. Assessment of mediastinal tumors with diffusion-weighted single-shot echo-planar MRI. *Journal of magnetic resonance imaging : JMRI* **2009**, *30*, 535-540, doi:10.1002/jmri.21871.
14. Sabri, Y.Y.; Nossair, E.Z.B.; Assal, H.H.; Wahba, H.S. Role of diffusion weighted MR-imaging in the evaluation of malignant mediastinal lesions. *Egyptian Journal of Radiology and Nuclear Medicine* **2020**, *51*, 32.
15. Huang, H.; Zhang, Y.; Cheng, J.; Wen, M. Whole-tumor histogram analysis of apparent diffusion coefficient maps in grading diagnosis of ependymoma. *Chinese Journal of Academic Radiology* **2020**, *2*, 41-46.
16. Donati, O.F.; Mazaheri, Y.; Afaq, A.; Vargas, H.A.; Zheng, J.; Moskowitz, C.S.; Hricak, H.; Akin, O. Prostate cancer aggressiveness: assessment with whole-lesion histogram analysis of the apparent diffusion coefficient. *Radiology* **2014**, *271*, 143-152.
17. Zhang, W.; Zhou, Y.; Xu, X.Q.; Kong, L.Y.; Xu, H.; Yu, T.F.; Shi, H.B.; Feng, Q. A Whole-Tumor Histogram Analysis of Apparent Diffusion Coefficient Maps for Differentiating Thymic Carcinoma from Lymphoma. *Korean journal of radiology* **2018**, *19*, 358-365, doi:10.3348/kjr.2018.19.2.358.